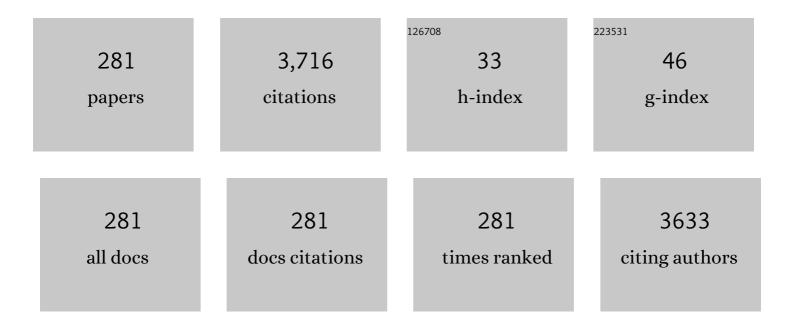
List of Publications by Year in descending order

Source: https://exaly.com/author-pdf/68781/publications.pdf Version: 2024-02-01



YOUNG-A SON

#	Article	IF	CITATIONS
1	Rhodamine-chloronicotinaldehyde-based "OFF–ON―chemosensor for the colorimetric and fluorescent determination of Al3+ ions. Sensors and Actuators B: Chemical, 2015, 208, 75-84.	4.0	87
2	A dual chemosensor for both Cu2+ and Al3+: A potential Cu2+ and Al3+ switched YES logic function with an INHIBIT logic gate and a novel solid sensor for detection and extraction of Al3+ ions from aqueous solution. Sensors and Actuators B: Chemical, 2016, 222, 447-458.	4.0	80
3	Synthesis of new TiO2/porphyrin-based composites and photocatalytic studies on methylene blue degradation. Dyes and Pigments, 2019, 160, 37-47.	2.0	79
4	Durable antimicrobial nylon 66 fabrics: Ionic interactions with quaternary ammonium salts. Journal of Applied Polymer Science, 2003, 90, 2194-2199.	1.3	76
5	Imparting durable antimicrobial properties to cotton fabrics using quaternary ammonium salts through 4-aminobenzenesulfonic acid–chloro–triazine adduct. European Polymer Journal, 2006, 42, 3059-3067.	2.6	74
6	Thermodynamic parameters of disperse dyeing on several polyester fibers having different molecular structures. Dyes and Pigments, 2005, 67, 229-234.	2.0	68
7	Efficient rhodamine-thiosemicarbazide-based colorimetric/fluorescent â€~turn-on' chemodosimeters for the detection of Hg2+ in aqueous samples. Sensors and Actuators B: Chemical, 2015, 214, 101-110.	4.0	67
8	Colorimetric and "turn-on―fluorescent determination of Hg2+ ions based on a rhodamine–pyridine derivative. Sensors and Actuators B: Chemical, 2014, 196, 388-397.	4.0	65
9	A highly selective dual-channel Cu2+ and Al3+ chemodosimeter in aqueous systems: Sensing in living cells and microfluidic flows. Sensors and Actuators B: Chemical, 2015, 210, 173-182.	4.0	65
10	A rhodamine scaffold immobilized onto mesoporous silica as a fluorescent probe for the detection of Fe (III) and applications in bio-imaging and microfluidic chips. Sensors and Actuators B: Chemical, 2016, 224, 404-412.	4.0	59
11	Uniform assembly of gold nanoparticles on S-doped g-C3N4 nanocomposite for effective conversion of 4-nitrophenol by catalytic reduction. Journal of Materials Science and Technology, 2020, 40, 176-184.	5.6	58
12	Effect of reactive anionic agent on dyeing of cellulosic fibers with a Berberine colorant. Dyes and Pigments, 2004, 60, 121-127.	2.0	57
13	Synthesis of novel squaraine–bis(rhodamine-6C): A fluorescent chemosensor for the selective detection of Hg2+. Sensors and Actuators B: Chemical, 2014, 202, 779-787.	4.0	54
14	A highly selective fluorescent chemosensor for Hg2+ based on a squaraine–bis(rhodamine-B) derivative: Part II. Sensors and Actuators B: Chemical, 2015, 210, 519-532.	4.0	54
15	AIE-active and reversible mechanochromic tetraphenylethene-tetradiphenylacrylonitrile hybrid luminogens with re-writable optical data storage application. Dyes and Pigments, 2017, 146, 7-13.	2.0	51
16	A reaction based colorimetric chemosensor for the detection of cyanide ion in aqueous solution. Sensors and Actuators B: Chemical, 2017, 246, 319-326.	4.0	49
17	A coumarin-derived Cu2+-fluorescent chemosensor and its direct application in aqueous media. Spectrochimica Acta - Part A: Molecular and Biomolecular Spectroscopy, 2018, 188, 571-580.	2.0	48
18	Effect of reactive anionic agent on dyeing of cellulosic fibers with a Berberine colorant—part 2: anionic agent treatment and antimicrobial activity of a Berberine dyeing. Dyes and Pigments, 2005, 64, 85-89.	2.0	47

#	Article	IF	CITATIONS
19	Prompt liquid-phase visual detection and low-cost vapor-phase detection of DCP, a chemical warfare agent mimic. Sensors and Actuators B: Chemical, 2016, 235, 447-456.	4.0	47
20	Tunable emission of hydrazine-containing bipyrrole fluorine–boron complexes by linear extension. Dyes and Pigments, 2016, 124, 232-240.	2.0	45
21	Highly selective naphthalimide-benzothiazole hybrid-based colorimetric and turn on fluorescent chemosensor for cyanide and tryptophan detection in aqueous media. Sensors and Actuators B: Chemical, 2018, 273, 143-152.	4.0	45
22	Ultrasonic synthesis of $\hat{l}\pm$ -MnO2 nanorods: An efficient catalytic conversion of refractory pollutant, methylene blue. Ultrasonics Sonochemistry, 2020, 62, 104870.	3.8	45
23	D–π–A solvatochromic charge transfer dyes containing a 2-cyanomethylene-3-cyano-4,5,5-trimethyl-2,5-dihydrofuran acceptor. Dyes and Pigments, 2010, 84, 169-175.	2.0	44
24	Efficient luminescence from easily prepared fluorine–boron core complexes based on benzothiazole and benzoxazole. Dyes and Pigments, 2014, 107, 182-187.	2.0	43
25	Rhodamine-fluorene based dual channel probe for the detection of Hg2+ ions and its application in digital printing. Sensors and Actuators B: Chemical, 2018, 261, 545-552.	4.0	43
26	Dual sensing performance of a rhodamine-derived scaffold for the determination of Cu2+ and Ce4+ in aqueous media. Sensors and Actuators B: Chemical, 2015, 220, 1254-1265.	4.0	42
27	Synthesis of near-infrared absorbing pyrylium-squaraine dye for selective detection of Hg2+. Sensors and Actuators B: Chemical, 2013, 188, 847-856.	4.0	41
28	Developing an RCB - Arduino device for the multi-color recognition, detection and determination of Fe(III), Co(II), Hg(II) and Sn(II) in aqueous media by a terpyridine moiety. Sensors and Actuators B: Chemical, 2019, 297, 126723.	4.0	40
29	Synthesis of azo and anthraquinone dyes and dyeing of nylon-6,6 in supercritical carbon dioxide. Journal of CO2 Utilization, 2020, 38, 49-58.	3.3	36
30	Synthesis and efficient dyeing of anthraquinone derivatives on polyester fabric with supercritical carbon dioxide. Dyes and Pigments, 2019, 166, 330-339.	2.0	35
31	Photoregulated optical switching of poly(N-isopropylacrylamide) hydrogel in aqueous solution with covalently attached spironaphthoxazine and D-ï€-A type pyran-based fluorescent dye. Dyes and Pigments, 2010, 87, 158-163.	2.0	34
32	Novel styrylbenzothiazolium dye-based sensor for mercury, cyanide and hydroxide ions. Spectrochimica Acta - Part A: Molecular and Biomolecular Spectroscopy, 2015, 144, 226-234.	2.0	34
33	Investigating Polaron Formation in Anatase and Brookite TiO ₂ by Density Functional Theory with Hybrid-Functional and DFT + <i>U</i> Methods. ACS Omega, 2019, 4, 8056-8064.	1.6	34
34	Porphyrin Dye/TiO2 imbedded PET to improve visible-light photocatalytic activity and organosilicon attachment to enrich hydrophobicity to attain an efficient self-cleaning material. Dyes and Pigments, 2019, 162, 8-17.	2.0	34
35	Optical properties of donor-Ï€-(acceptor)n merocyanine dyes with dicyanovinylindane as acceptor group and triphenylamine as donor unit. Dyes and Pigments, 2009, 82, 293-298.	2.0	33
36	Photophysical, electrochemical, thermal and aggregation properties of new metal phthalocyanines. Journal of Molecular Structure, 2017, 1147, 469-479.	1.8	33

#	Article	IF	CITATIONS
37	Berberine finishing for developing antimicrobial nylon 66 fibers: % exhaustion, colorimetric analysis, antimicrobial study, and empirical modeling. Journal of Applied Polymer Science, 2007, 103, 1175-1182.	1.3	32
38	A colorimetric and fluorometric chemosensor for the selective detection of cyanide ion in both the aqueous and solid phase. Sensors and Actuators B: Chemical, 2017, 253, 942-948.	4.0	29
39	Tuning of the Topochemical Polymerization of Diacetylenes Based on an Odd/Even Effect of the Peripheral Alkyl Chain: Thermochromic Reversibility in a Thin Film and a Single-Component Ink for a Fountain Pen. ACS Applied Materials & Interfaces, 2018, 10, 24767-24775.	4.0	29
40	A diaminomaleonitrile-appended BODIPY chemosensor for the selective detection of Cu2+ via oxidative cyclization and imaging in SiHa cells and zebrafish. Spectrochimica Acta - Part A: Molecular and Biomolecular Spectroscopy, 2020, 233, 118179.	2.0	29
41	An approach to the dyeing of polyester fiber using indigo and its extended wash fastness properties. Dyes and Pigments, 2004, 61, 263-272.	2.0	28
42	An â€~OFF–ON' fluorescent chemosensor based on rhodamine 6G-2-chloronicotinaldehyde for the detection of Al3+ ions: Part II. Sensors and Actuators B: Chemical, 2016, 227, 227-241.	4.0	27
43	A benzothiazole-based semisquarylium dye suitable for highly selective Hg2+ sensing in aqueous media. Dyes and Pigments, 2009, 83, 324-327.	2.0	26
44	Liquid and gaseous state visual detection of chemical warfare agent mimic DCP by optical sensor. Dyes and Pigments, 2019, 171, 107712.	2.0	26
45	Ultrasound-assisted method to improve the structure of CeO2@polyprrole core-shell nanosphere and its photocatalytic reduction of hazardous Cr6+. Ultrasonics Sonochemistry, 2019, 59, 104738.	3.8	26
46	Synthesis and property of solvatochromic fluorophore based on D-Ï€-A molecular system: 2-{[3-Cyano-4-(N-ethyl-N-(2-hydroxyethyl)amino)styryl]-5,5-dimethylfuran-2(5H)-ylidene}malononitrile dye. Spectrochimica Acta - Part A: Molecular and Biomolecular Spectroscopy, 2010, 75, 225-229.	2.0	25
47	A renovation of non-aqueous Al3+ sensor to aqueous media sensor by simple recyclable immobilize electrospun nano-fibers and its uses for live sample analysis. Sensors and Actuators B: Chemical, 2016, 228, 259-269.	4.0	25
48	A simple and fast responsive colorimetric moisture sensor based on symmetrical conjugated polymer. Sensors and Actuators B: Chemical, 2020, 311, 127906.	4.0	25
49	The synthesis and proton-induced spectral switching of a novel azine dye and its boron complex. Dyes and Pigments, 2010, 87, 268-271.	2.0	24
50	Toggle-switchable fluorescence of bisindolylmaleimide derivatives by reversible esterification/hydrolysis. Tetrahedron Letters, 2012, 53, 1098-1101.	0.7	24
51	A new rhodamine 6 G based chemosensor for trace level Al3+ and its thin film application in 100% aqueous medium. Sensors and Actuators B: Chemical, 2016, 236, 184-191.	4.0	24
52	Synthesis of novel reactive disperse dyes comprising carbamate and cyanuric chloride groups for dyeing polyamide and cotton fabrics in supercritical carbon dioxide. Dyes and Pigments, 2022, 198, 110003.	2.0	24
53	The photo- and electrophysical properties of curcumin in aqueous solution. Spectrochimica Acta - Part A: Molecular and Biomolecular Spectroscopy, 2010, 76, 384-387.	2.0	23
54	The dyeing of supermicrofibre nylon with acid and vat dyes. Dyes and Pigments, 2010, 87, 132-138.	2.0	23

#	Article	IF	CITATIONS
55	An anion sensor based on the displacement of 2,6-dichlorophenol-indo-o-cresol sodium salt from a water-soluble tetrasulfonated calix[4]arene. Dyes and Pigments, 2011, 88, 84-87.	2.0	23
56	Imidazole-containing ratiometric receptor for the selective and sensitive detection of cyanide and fluoride via deprotonation and a receptor-anion ensemble for Cu2+ sensing. Journal of Luminescence, 2018, 204, 244-252.	1.5	22
57	Investigation of reversible self-thermochromism in microencapsulated fluoran-based materials. Dyes and Pigments, 2018, 151, 64-74.	2.0	21
58	Affinity of disperse dyes on poly(ethylene terephthalate) in non-aqueous media. Part 2: effect of substituents. Dyes and Pigments, 2005, 66, 19-25.	2.0	20
59	Through-bond energy transfer based dyad and triad shape fluorescence "OFF-ON-OFF―probes for Hg2+ ions and their application in live HeLa cells and Zebrafish. Sensors and Actuators B: Chemical, 2017, 240, 1272-1282.	4.0	20
60	Development of naphthalimide-functionalized thermochromic conjugated polydiacetylenes and their reversible green-to-red chromatic transition in the solid state. Dyes and Pigments, 2019, 164, 355-362.	2.0	20
61	Fabrication and topochemically controlled diacetylene-based polymer and its colorimetric application toward HCl detection. Dyes and Pigments, 2020, 174, 108061.	2.0	20
62	The fastness, to repeated washing, of reactive dyes and pre-metallised acid dyes on nylon 6,6. Dyes and Pigments, 2000, 45, 43-49.	2.0	19
63	A highly selective and sensitive photoswitchable fluorescent probe for Hg2+ based on bisthienylethene–rhodamine 6G dyad and for live cells imaging. Spectrochimica Acta - Part A: Molecular and Biomolecular Spectroscopy, 2014, 128, 567-574.	2.0	19
64	Catalytic performance of graphene quantum dot supported manganese phthalocyanine for efficient oxygen reduction: density functional theory approach. New Journal of Chemistry, 2019, 43, 348-355.	1.4	19
65	Spontaneous optical response towards cyanide ion in water by a reactive binding site probe. Spectrochimica Acta - Part A: Molecular and Biomolecular Spectroscopy, 2020, 233, 118190.	2.0	19
66	Do HOMO–LUMO Energy Levels and Band Gaps Provide Sufficient Understanding of Dye-Sensitizer Activity Trends for Water Purification?. ACS Omega, 2020, 5, 15052-15062.	1.6	18
67	Thermodynamic analysis of 1,4-diaminoanthraquinone adsorption on polyethylene terephthalate in alkane media. Dyes and Pigments, 2007, 72, 246-250.	2.0	17
68	The synthesis and spectral properties of a stimuli-responsive D–̀–A charge transfer dye based on indole donor and 2-cyanomethylene-3-cyano-4,5,5-trimethyl-2,5-dihydrofuran acceptor moieties. Journal of Photochemistry and Photobiology A: Chemistry, 2011, 217, 224-227.	2.0	17
69	A novel sensing capabilities and structural modification from thiourea to urea derivative by Hg(ClO4)2: Selective dual chemodosimeter for Hg2+ and Fâ ^{^,} ions. Sensors and Actuators B: Chemical, 2015, 220, 1070-1085.	4.0	17
70	Michael addition-based colorimetric and fluorescence chemodosimeters for the nanomolar-level tracking of cyanide ions in aqueous-organic media. Sensors and Actuators B: Chemical, 2016, 237, 341-349.	4.0	17
71	Synthesis and characterization of triphenylamine-based polymers and their application towards solid-state electrochromic cells. RSC Advances, 2016, 6, 78984-78993.	1.7	17
72	Porphyrin dye/TiO2 entrenched in PET to attain self-cleaning property through visible light photocatalytic activity. Research on Chemical Intermediates, 2019, 45, 3655-3671.	1.3	17

#	Article	IF	CITATIONS
73	New pH indicator based on 1,3-bisdicyanovinylindane. Dyes and Pigments, 2005, 64, 153-155.	2.0	16
74	Synthesis and chemosensitivity of a new iminium salt toward a cyanide anion. Spectrochimica Acta - Part A: Molecular and Biomolecular Spectroscopy, 2014, 127, 268-274.	2.0	16
75	A comparison of the optical and photovoltaic properties of novel double branched organic dyes in dye sensitized solar cells. Synthetic Metals, 2015, 203, 235-242.	2.1	16
76	Design and synthesis of polydiacetylenes, and their low temperature irreversible thermochromic properties. Dyes and Pigments, 2021, 184, 108839.	2.0	16
77	Affinity of disperse dyes on poly(ethylene terephthalate) in non-aqueous media: part 1. Adsorption and solubility properties. Dyes and Pigments, 2005, 64, 73-78.	2.0	15
78	Synthesis and Characterization of Quinoline-based Dye Sensor. Molecular Crystals and Liquid Crystals, 2009, 504, 173-180.	0.4	15
79	A BODIPY based highly selective fluorescence turn-on sensor toward VIB and IIB metal ions. Molecular Crystals and Liquid Crystals, 2016, 636, 159-167.	0.4	15
80	Synthesis, thermochromic, solvatochromic and axial ligation studies of Zn-porphyrin complex. Inorganica Chimica Acta, 2018, 469, 453-460.	1.2	15
81	A BODIPY based emission signal turn-on probe toward multiple heavy metals. Molecular Crystals and Liquid Crystals, 2020, 706, 38-46.	0.4	15
82	Effect of phenyl ring substitution on J-aggregate formation ability of novel bisazomethine dyes in vapour-deposited films. Dyes and Pigments, 2011, 90, 56-64.	2.0	14
83	Spectral Switching of Naphthalimide-Coumarin Induced by F–. Journal of Nanoscience and Nanotechnology, 2015, 15, 5370-5373.	0.9	14
84	A new dual fluorogenic and chromogenic "turn-on―chemosensor for Cu2+/Fâ^' ions. Spectrochimica Acta - Part A: Molecular and Biomolecular Spectroscopy, 2015, 151, 48-55.	2.0	14
85	Synthesis of fluorescent cationic coumarin dyes with rigid molecular structures to improve lightfastness and their related modacrylic dyed fibers. Dyes and Pigments, 2021, 190, 109294.	2.0	14
86	The thermoresponsive behaviour of a poly(N-isopropylacrylamide) hydrogel with a D-Ï€-A type pyran-based fluorescent dye. Dyes and Pigments, 2010, 87, 84-88.	2.0	13
87	The synthesis and spectral properties of a stimuli-responsive D-Ï€-A charge transfer dye. Spectrochimica Acta - Part A: Molecular and Biomolecular Spectroscopy, 2011, 78, 234-237.	2.0	13
88	Design and synthesis of novel chemosensor based on rhodamine 6G monitoring heavy metal ions. Supramolecular Chemistry, 2013, 25, 87-91.	1.5	12
89	"Turn-on―fluorescent and colorimetric determination of Cu2+ ions in aqueous media based on a Rhodamine-N-phenyl Semicarbazide derivative. Fibers and Polymers, 2015, 16, 953-960.	1.1	12
90	Nitro Substituted Bisindolylmalimide Derivatives: Position-Dependent Emission. Molecular Crystals and Liquid Crystals, 2015, 608, 273-281.	0.4	12

#	Article	IF	CITATIONS
91	Synthesis of a novel pyrylium salt with chemoselectivity to a cyanide anion. Supramolecular Chemistry, 2015, 27, 191-200.	1.5	12
92	Thiophene Modulated BODIPY Dye as a Light Harvester. Molecular Crystals and Liquid Crystals, 2019, 679, 127-136.	0.4	12
93	Selective detection of cyanide ion in 100 % water by indolium based dual reactive binding site optical sensor. Journal of Photochemistry and Photobiology A: Chemistry, 2020, 397, 112571.	2.0	12
94	Synthesis and characterisation of new acridine dye molecules combined UV absorber and exploring photophysical properties. Dyes and Pigments, 2021, 192, 109391.	2.0	12
95	An ecofriendly dyeing of nylon and cotton fabrics in supercritical CO2 with novel tricyanopyrrolidone reactive disperse dye. Journal of CO2 Utilization, 2022, 60, 102004.	3.3	12
96	Facile Preparation of Biopatternable Surface for Selective Immobilization from Bacteria to Mammalian Cells. Journal of Nanoscience and Nanotechnology, 2009, 9, 1204-1209.	0.9	11
97	Effects of alkoxy substitution on the crystal structure of 2,3-bis[(E)-4-(diethylamino)-2-alkoxybenzylideneamino]fumaronitrile derivatives. CrystEngComm, 2011, 13, 5374.	1.3	11
98	Design, Synthesis and Optical Property of Rhodamine 6G Based New Dye Sensor. Molecular Crystals and Liquid Crystals, 2012, 566, 45-53.	0.4	11
99	Fast ethylamine gas sensing based on intermolecular charge-transfer complexation. Chinese Chemical Letters, 2012, 23, 484-487.	4.8	11
100	Modulation of a fluorescence switch of nanofiber mats containing photochromic spironaphthoxazine and D-ï€-A charge transfer dye. Journal of Luminescence, 2012, 132, 1427-1431.	1.5	11
101	Properties of Star Shaped Thiophene Materials Having a Build-In Photochromic Core. Molecular Crystals and Liquid Crystals, 2014, 602, 1-8.	0.4	11
102	Synthesis of porphyrin sensitizers with a thiazole group as an efficient π-spacer: potential application in dye-sensitized solar cells. RSC Advances, 2016, 6, 41294-41303.	1.7	11
103	Solvent effect on the thermochromism of new betaine dyes. Dyes and Pigments, 2017, 136, 458-466.	2.0	11
104	Chemically interconnected ternary AgNP/polypyrrole/functionalized buckypaper composites as high-energy-density supercapacitor electrodes. Chemical Physics Letters, 2020, 739, 136957.	1.2	11
105	Squarylium-based chromogenic anion sensors. Spectrochimica Acta - Part A: Molecular and Biomolecular Spectroscopy, 2012, 95, 25-28.	2.0	10
106	Optical properties of novel pyrene fluoric chemosensor toward fluoride anions. Fibers and Polymers, 2013, 14, 2010-2014.	1.1	10
107	Solvent Dependent Energy Transfer ofN-bridged Naphthalimide-Bisindolymaleimide Fluorescent Dyes. Molecular Crystals and Liquid Crystals, 2013, 584, 18-26.	0.4	10
108	"Turn-On―Fluorescent and Colorimetric Detection of Zn ²⁺ lons by Rhodamine-Cinnamaldehyde Derivative. Journal of Nanoscience and Nanotechnology, 2018, 18, 5333-5340.	0.9	10

#	Article	IF	CITATIONS
109	A BODIPY-based highly emissive dye with thiophene-based branch harvesting the light. Molecular Crystals and Liquid Crystals, 2018, 662, 157-164.	0.4	10
110	Electrochemical Oxygen-Reduction Activity and Carbon Monoxide Tolerance of Iron Phthalocyanine Functionalized with Graphene Quantum Dots: A Density Functional Theory Approach. Journal of Physical Chemistry C, 2019, 123, 27483-27491.	1.5	10
111	DPP based dual-sensing probe for the multi-color detection of toxic Co2+/Sn2+ and CNâ^ ions in water: An electronic eye development. Dyes and Pigments, 2021, 192, 109425.	2.0	10
112	Synthesis of novel panchromatic porphyrin-squaraine dye and application towards TiO2 combined photocatalysis. Journal of Photochemistry and Photobiology A: Chemistry, 2020, 397, 112595.	2.0	10
113	Colorimetric signaling of mono-, di-, and triethylamine based on intermolecular n-ï€ charge transfer interaction. Fibers and Polymers, 2009, 10, 855-857.	1.1	9
114	Synthesis and Optical Chromic Properties of New Barbituric Acid based Dye Molecules Having Push-Ï€-Pull System. Molecular Crystals and Liquid Crystals, 2011, 550, 240-249.	0.4	9
115	Ac ₂ O/HCl Modulated Fluorescence On–Off Model Based on Arylmaleimide. Journal of Nanoscience and Nanotechnology, 2015, 15, 5366-5369.	0.9	9
116	Photo discoloration of eosin yellow dye under visible light using TiO2@TPPS nanocomposite synthesized via ultrasonic assisted method. Colloids and Surfaces A: Physicochemical and Engineering Aspects, 2021, 608, 125601.	2.3	9
117	A novel near-infrared fluorescent probe for rapid detection of peroxynitrite with large stokes shift and imaging in living cells. Journal of Photochemistry and Photobiology A: Chemistry, 2022, 423, 113579.	2.0	9
118	Degradation of the disazo acid dye by the sulfur-containing amino acids of wool fibers. Dyes and Pigments, 2005, 67, 127-132.	2.0	8
119	Indigo adsorption properties to polyester fibers of different levels of fineness. Dyes and Pigments, 2005, 65, 137-143.	2.0	8
120	Self-assembly multi-layer of diazonium resin and its coupling reaction with J-acid and H-acid. Dyes and Pigments, 2007, 72, 345-348.	2.0	8
121	New fluorescent dye chemosensor for mercury ion (Hg2+) detection. Fibers and Polymers, 2009, 10, 272-274.	1.1	8
122	Synthesis and Solvatofluorochromism Behaviors on Intramolecular Charge Transfer System of Novel D-ï€-A Dyes. Molecular Crystals and Liquid Crystals, 2012, 563, 257-271.	0.4	8
123	Deprotonation/Protonation Induced Spectral Switching of 1,8-Naphthalimide Dye. Molecular Crystals and Liquid Crystals, 2014, 600, 163-169.	0.4	8
124	Through-Bond Energy Transfer Cassettes: Pyrene-Bisindolylmaleimide Dyads with Large Pseudo-Stokes Shifts. Molecular Crystals and Liquid Crystals, 2014, 601, 182-189.	0.4	8
125	Rhodamineâ€based Colorimetric and Fluorescent Chemosensors for the Detection of Cu ²⁺ Ions and its Application to Bioimaging. Bulletin of the Korean Chemical Society, 2018, 39, 972-981.	1.0	8
126	Configuration of white light emission by courmarin and naphthalimide. Molecular Crystals and Liquid Crystals, 2018, 660, 10-16.	0.4	8

#	Article	IF	CITATIONS
127	A Novel Morpholine-Based Rhodamine Fluorescent Chemosensor for the Rapid Detection of Hg ²⁺ Ions. Journal of Nanoscience and Nanotechnology, 2019, 19, 6893-6898.	0.9	8
128	Visible Light Photo-Sensitized Metallo-Porphyrin/TiO2 Photocatalyst and Its Related Self-Cleaning Effects in Poly Ethylene Terephthalate. Journal of Nanoscience and Nanotechnology, 2019, 19, 8004-8012.	0.9	8
129	A photocatalytic comparison study between tin complex and carboxylic acid derivatives of porphyrin/TiO2 composites. Research on Chemical Intermediates, 2020, 46, 313-328.	1.3	8
130	Emission shift of an imidazole bridged diethylaminocoumarin and diphenyl. Molecular Crystals and Liquid Crystals, 2020, 704, 48-56.	0.4	8
131	Controlled ultrasonic synthesis of TiO2@C3N4 nanocomposites with porphyrin as a solid-state electron mediator: A promising material for pollutant discoloration under visible light. Ceramics International, 2021, 47, 14399-14407.	2.3	8
132	Rhodamine 6G Based New Fluorophore Chemosensor Toward Hg ²⁺ . Textile Coloration and Finishing, 2012, 24, 158-164.	0.0	8
133	Synthesis of a novel bridge compound having hetero-bi-functional reactive groups. Part 2: the characteristics of disperse dyeings. Dyes and Pigments, 2005, 66, 27-32.	2.0	7
134	Benzothiazole-based semisquaraine as colorimetric chemosensor for Hg2+. Fibers and Polymers, 2009, 10, 403-405.	1.1	7
135	Luminescence switching of CdTe quantum dots in presence of water-soluble spironaphthoxazine. Spectrochimica Acta - Part A: Molecular and Biomolecular Spectroscopy, 2012, 97, 699-702.	2.0	7
136	Optical properties of photo- and thermo-responsive aqueous CdTe quantum dots/spironaphthoxazine/poly(N-isopropylacrylamide) hybrid. Spectrochimica Acta - Part A: Molecular and Biomolecular Spectroscopy, 2012, 97, 806-810.	2.0	7
137	Benzothiazole and indole based dye sensor: Optical switching functions with pH stimuli. Fibers and Polymers, 2012, 13, 1101-1104.	1.1	7
138	Switching properties of fluorescent photochromic poly(methyl methacrylate) with spironaphthoxazine and D-l€-A type pyran-based fluorescent dye. Spectrochimica Acta - Part A: Molecular and Biomolecular Spectroscopy, 2012, 86, 600-604.	2.0	7
139	Chromene and Imidazole Based <i>D-ï€-A</i> Chemosensor Preparation and Its Anion Responsive Effects. Molecular Crystals and Liquid Crystals, 2014, 599, 16-22.	0.4	7
140	Synthesis, characterization and aggregation and fluorescence properties of novel highly soluble zinc phthalocyanines bearing tetrakis-4-(3-(piperidin-1-yl)phenoxy) with tetra and dodecachloro substituents. Fibers and Polymers, 2016, 17, 553-559.	1.1	7
141	Naphthalimide-coumarin: Dependent energy transfer cassette and its response to Fâ^'. Molecular Crystals and Liquid Crystals, 2017, 644, 257-266.	0.4	7
142	Emission behavior of perimidine attached BODIPY and its response to acid/base. Molecular Crystals and Liquid Crystals, 2017, 654, 131-138.	0.4	7
143	Dye Clicked Thermoplastic Polyurethane as a Generic Platform toward Chromic-Polymer Applications. Scientific Reports, 2019, 9, 18648.	1.6	7
144	A Chromone Based Fluorescent Probe for the Effective Detection of Aluminium Ion. Journal of Nanoscience and Nanotechnology, 2020, 20, 2840-2846.	0.9	7

#	Article	IF	CITATIONS
145	An "electron lock―toward the photochromic activity of phenylacetylene appended bisthienylethene. Molecular Crystals and Liquid Crystals, 2020, 706, 141-149.	0.4	7
146	Ultrasonic assisted fabrication of dual function surface on PET and preparation of single component ink to attain efficient self-cleaning function via digital printing. Journal of Molecular Liquids, 2021, 324, 114668.	2.3	7
147	A New Anthracene Based Fluorescent Turn-On Sensor for Fe ³⁺ . Bulletin of the Korean Chemical Society, 2014, 35, 277-279.	1.0	7
148	Electrochemical Study on Rhodamine 6G-Indole Based Dye for HOMO and LUMO Energy Levels. Textile Coloration and Finishing, 2013, 25, 7-12.	0.0	7
149	A novel class of xanthene dyes with chemically linked UV absorber molecule and their photophysical properties. Spectrochimica Acta - Part A: Molecular and Biomolecular Spectroscopy, 2022, 279, 121437.	2.0	7
150	Electro-Optical Properties and X-ray Crystal Structure of a New Bisazomethine Dye. Molecular Crystals and Liquid Crystals, 2008, 492, 46/[410]-55/[419].	0.4	6
151	Synthesis and optical/chemical properties of triphenylamine derivatives based mono-, di-, and tri-indanedione. Fibers and Polymers, 2009, 10, 739-742.	1.1	6
152	Deprotonation/protonationâ€induced spectral switching of naphthalimideâ€coumarin chromophore. Physica Status Solidi C: Current Topics in Solid State Physics, 2012, 9, 2456-2459.	0.8	6
153	Significant emission red-shift of BODIPY derivatives with strong electron-acceptor attached. Molecular Crystals and Liquid Crystals, 2017, 654, 139-145.	0.4	6
154	Synthesis of a new phenothiazine-carbazole polymer derivative and utilization in an electrochromic cell. Synthetic Metals, 2018, 240, 1-7.	2.1	6
155	2,4-Dimethylpyrrole Configured Fluorine-Boron Complexes. Molecular Crystals and Liquid Crystals, 2018, 677, 34-41.	0.4	6
156	Synthesis of novel betaine dyes for multi chromic sensors. Journal of Molecular Structure, 2019, 1187, 151-163.	1.8	6
157	Robust Photodegradation of Methylene Blue with the Biphenyl-Porphyrin/TiO ₂ Photocatalyst Under Visible Light Condition. Journal of Nanoscience and Nanotechnology, 2020, 20, 6266-6273.	0.9	6
158	A Photochromic Fluorescent Probe for Hg ² ⁺ Based on Dithienylethene-Rhodamine B Dyad and Its Application in Live Cells Imaging. Science of Advanced Materials, 2017, 9, 533-540.	0.1	6
159	Synthesis of a novel bridge compound having hetero-bi-functional reactive groups. Part 1: its adsorption properties. Dyes and Pigments, 2005, 65, 261-266.	2.0	5
160	An anion sensor based on calix[4]arene-Reichardt's dye. Fibers and Polymers, 2009, 10, 858-860.	1.1	5
161	Isophorone and pyrrole based push-pull system dye: Design, preparation and spectral switching on pH/fluoride ion. Fibers and Polymers, 2011, 12, 692-695.	1.1	5
162	A Colorimetric and Fluorescent Chemosensor for Ni ²⁺ Based on Donor- <i>ï€</i> -Acceptor Charge Transfer Dye Containing 2-Cyanomethylene-3-Cyano-4,5,5-Trimethyl-2,5-Dihydrofuran Acceptor and 4-Bis(pyridin-2-ylmethyl)Aminobenzene Donor. Journal of Nanoscience and Nanotechnology, 2012, 12, 1503-1506.	0.9	5

#	Article	IF	CITATIONS
163	Fluorescence quenching of carbazole by 2-chloro-3,5-dinitrobenzotrifluoride-ethylamines intermolecular charge-transfer complex. Spectrochimica Acta - Part A: Molecular and Biomolecular Spectroscopy, 2013, 103, 453-455.	2.0	5
164	A Highly Selective Rhodamine Based Colorimetric Sensor Toward Cu ²⁺ . Molecular Crystals and Liquid Crystals, 2014, 599, 8-15.	0.4	5
165	Investigation of a Naphthalimide Based OH ^{â^'} Sensor with Quinoline Attached. Molecular Crystals and Liquid Crystals, 2015, 622, 84-93.	0.4	5
166	The effect of terminal dimethyl and diethyl substituents on the J-aggregate-like molecular arrangement of bisazomethine dye molecules. CrystEngComm, 2015, 17, 7213-7226.	1.3	5
167	Synthesis and characterization of tetra phenoxy-substituted halogen-rich metallophthalocyanine derivatives: A study on their LCD color filter requirements. Journal of Molecular Structure, 2016, 1119, 325-331.	1.8	5
168	Optical Properties of 1,3-Bisdicyanovinylindane, an Electro-Acceptor, Attached Bisthienylethene Molecule. Journal of Nanoscience and Nanotechnology, 2016, 16, 1752-1755.	0.9	5
169	Absorption and emission investigation of boron-cored dye. Molecular Crystals and Liquid Crystals, 2017, 659, 64-70.	0.4	5
170	Thermally Reversible Fluorans: Synthesis, Thermochromic Properties and Real Time Application. Journal of Nanoscience and Nanotechnology, 2018, 18, 3299-3305.	0.9	5
171	Reversed photochromism reactivity of malononitrile attached bisthienylthene. Molecular Crystals and Liquid Crystals, 2018, 662, 147-156.	0.4	5
172	Photochromic reactivity induced by electron distribution: active or inactive. Molecular Crystals and Liquid Crystals, 2019, 689, 83-91.	0.4	5
173	Acridine-based fluorophores with improved lightfastness properties. Dyes and Pigments, 2022, 197, 109924.	2.0	5
174	A Pyrene-Tetrazole Fused Fluorescent Probe for Effective Real Time Detection Towards Aluminium Ion. Journal of Fluorescence, 2022, 32, 1703-1712.	1.3	5
175	Development of berberine attraction sites onto cellulosic substrates modified by reactive bridging agent: Statistical optimization and analysis. Colloids and Surfaces A: Physicochemical and Engineering Aspects, 2008, 325, 120-126.	2.3	4
176	Synthesis and Spectral Properties of a Highly Selective D-Ï€-A Based Dye Chemosensor. Molecular Crystals and Liquid Crystals, 2011, 538, 327-332.	0.4	4
177	Spectroscopic Characterization of Heptamethine Cyanine Dyes for the Interaction with the CN-and F Molecular Crystals and Liquid Crystals, 2012, 566, 61-66.	0.4	4
178	Solvent Dependent Triphenylamine Based D-(Ï€-A)n Type Dye Molecules and Optical Properties. Journal of Nanoscience and Nanotechnology, 2012, 12, 1497-1502.	0.9	4
179	Temperature-modulated quenching and photoregulated optical switching of poly(N-isopropylacrylamide)/spironaphthoxazine/Rhodamine B hybrid in water. Spectrochimica Acta - Part A: Molecular and Biomolecular Spectroscopy, 2012, 94, 308-311.	2.0	4
180	Properties and characteristics of squarylium-based chemosensors for Hg2+. Supramolecular Chemistry, 2013, 25, 61-64.	1.5	4

#	Article	IF	CITATIONS
181	F ^{â^'} /OH ^{â^'} Triggered Optical Switching Functions of Naphthalimide Chromophoric Materials. Molecular Crystals and Liquid Crystals, 2014, 604, 184-192.	0.4	4
182	A Highly Sensitive Fluorescent Probe for Selective Detection of Al ³⁺ Cation by Switching the Solvent from Aprotic to Protic Environment. Molecular Crystals and Liquid Crystals, 2015, 622, 103-113.	0.4	4
183	Synthesis, characterization, and photocatalytic disinfection studies of porphyrin dimer/TiO2-based photocatalyst. Journal of Molecular Structure, 2021, 1236, 130276.	1.8	4
184	A novel polymeric hybrid sensory smart material for the prompt recognition of mercury ions in water. Microchemical Journal, 2021, 170, 106707.	2.3	4
185	Effect of UV, pH and solvent on the photophysical properties of novel xanthylium fluorophore in solid and liquid state. Dyes and Pigments, 2022, 205, 110480.	2.0	4
186	Preparation of luminescing nanocrystal and its application to electrospinning. Fibers and Polymers, 2008, 9, 534-537.	1.1	3
187	Characterization of Acetylacetonato-bis-(2-(4-amino-2-hydroxyphenyl)benzthiazole) Complex. Molecular Crystals and Liquid Crystals, 2009, 498, 151-157.	0.4	3
188	Synthesis of 2,2-bithiophene Based Dye Sensor and Optical Properties Toward Metal Cations. Molecular Crystals and Liquid Crystals, 2011, 551, 163-171.	0.4	3
189	Characteristics of Guajazulene Based Chemosensor Toward CN ^{â^'} and F ^{â^'} Anions. Molecular Crystals and Liquid Crystals, 2014, 600, 189-195.	0.4	3
190	A highly selective rhodamine based color turn on and fluorescence turn off sensor toward late IB metal ions. Fibers and Polymers, 2014, 15, 914-917.	1.1	3
191	Synthesis and characterization of water-soluble phthalocyanine Copper(II) complex and its coloration on acrylic fibers. Fibers and Polymers, 2015, 16, 2552-2557.	1.1	3
192	The excited-state intramolecular proton transfer fluorescence of HBT derivative induced by solvent polarity. Molecular Crystals and Liquid Crystals, 2016, 635, 158-166.	0.4	3
193	Charge transfer modulated photochromic reactivity by incorporation picolylamine to a diarylethene unit. Molecular Crystals and Liquid Crystals, 2016, 636, 1-9.	0.4	3
194	A Novel Fluorescent Chemosensor Based on β-(2-Pyridyl)acrolein-Rhodamine B Derivative: Polymer Particle Interaction with an Enhanced Sensing Performance. KONA Powder and Particle Journal, 2016, 33, 228-238.	0.9	3
195	High Pseduo-Stoke's Shift of a Naphthalene-Bisindolylmaleimide Dye. Journal of Nanoscience and Nanotechnology, 2016, 16, 856-860.	0.9	3
196	Synthesis of octa-phenoxy substituted metallophthalocyanines and their green color filter application in liquid crystal display. Molecular Crystals and Liquid Crystals, 2017, 644, 88-97.	0.4	3
197	Electrochemical, Photophysical and Theoretical Studies of Novel Zinc Phthalocyanines. Journal of Nanoscience and Nanotechnology, 2020, 20, 5402-5410.	0.9	3
198	Simple easy to make xanthene based optical probe for solid and liquid state Hg2+ ion detection. Spectrochimica Acta - Part A: Molecular and Biomolecular Spectroscopy, 2022, 266, 120413.	2.0	3

#	Article	IF	CITATIONS
199	Highly visible bis-heterocyclic acridinium and xanthenium-based dyes: Synthesis, AIEE, and modacrylic dyeing. Dyes and Pigments, 2022, 200, 110159.	2.0	3
200	Ultrasonic assisted surface modified cellulose: Photocatalytic effect for the disinfection of microbes using porphyrin dyes. Dyes and Pigments, 2022, 204, 110393.	2.0	3
201	Multi-layer preparation of phthalocyanine dye and diazonium resin using a self-assembly fabrication method. Journal of Porphyrins and Phthalocyanines, 2006, 10, 991-995.	0.4	2
202	Polymethine Dye Synthesis and Its Leuco Property Investigation. Molecular Crystals and Liquid Crystals, 2007, 472, 225/[615]-230/[620].	0.4	2
203	Crystal structure of 4-formylphenyl-diphenylamine, C19H15NO. Zeitschrift Fur Kristallographie - New Crystal Structures, 2009, 224, 459-460.	0.1	2
204	Dye Chemosensing Effect and Characterization Based on Hydroxyl Anthracene and Naphthalene Moiety. Molecular Crystals and Liquid Crystals, 2010, 519, 90-98.	0.4	2
205	Synthesis and Characterization of Benz-X-azole Based Dye Chemosensor. Molecular Crystals and Liquid Crystals, 2010, 519, 99-107.	0.4	2
206	Synthesis and optical properties of a naphthalimide dimer. Physica Status Solidi C: Current Topics in Solid State Physics, 2012, 9, 2452-2455.	0.8	2
207	A BisindolyImaleimide–Naphthalimide Building Block for the Construction of the Energy Transfer Cassette. Journal of Nanoscience and Nanotechnology, 2014, 14, 8033-8037.	0.9	2
208	Synthesis, Optical, Electrochemical and Theoretical Studies of New Multicyclic Substituted Phthalocyanines. Journal of Nanoscience and Nanotechnology, 2018, 18, 3192-3205.	0.9	2
209	Emission behavior of naphthalimide-coumarin cassette. Molecular Crystals and Liquid Crystals, 2018, 662, 139-146.	0.4	2
210	Synthesis, Generic Dyeing of Nindigo Derivatives on Unmodified Polypropylene; First Time Application in Dyeing Technology. Journal of Nanoscience and Nanotechnology, 2019, 19, 7105-7111.	0.9	2
211	Shifting the emission of proton transfer fluorescence with fluorine-boron as the rotation lock. Molecular Crystals and Liquid Crystals, 2020, 704, 41-47.	0.4	2
212	Crystal structure of 5,5',5''-tribromo-3,3''-dimethyl-2,2':3',2''- terthiophene, C14H9Br3S3. Zeitschrift Fur Kristallographie - New Crystal Structures, 2009, 224, 697-698.	0.1	2
213	Electrochemical Study for 1,3-Bisdicyanovinylindane. Textile Coloration and Finishing, 2013, 25, 89-93.	0.0	2
214	Development of Cationic Dyeable Polyamide Substrates by Pretreatment with Synthetic Tanning Agent: Statistical Optimization and Analysis. Textile Coloration and Finishing, 2009, 21, 41-50.	0.0	2
215	Solvatochromism of indonaphthol dye. Fibers and Polymers, 2008, 9, 659-660.	1.1	1
216	Self-Assembly Fabrication Using Diazo Coupling Dye and Spiroxazine. Molecular Crystals and Liquid Crystals, 2008, 491, 94-102.	0.4	1

#	Article	IF	CITATIONS
217	Crystal structure of 2,3-bis(5-bromo-3-methylthiophen-2- yl)benzo[b]thiophene, C18H12Br2S3. Zeitschrift Fur Kristallographie - New Crystal Structures, 2009, 224, 691-692.	0.1	1
218	Synthesis and Optical Properties of (A) _n - ï€ -(Ph) ₃ N Type Dyes. Molecular Crystals and Liquid Crystals, 2009, 504, 164-172.	0.4	1
219	Self-assembly layer-by-layer fabrication using porphyrin dye anion and polycation. Journal of Porphyrins and Phthalocyanines, 2009, 13, 774-778.	0.4	1
220	Characterization of New Benz-X-Azole Dye Derivatives and Metal Complexes. Molecular Crystals and Liquid Crystals, 2009, 498, 158-164.	0.4	1
221	Synthesis and Sensing Properties of Triphenylamine Based Dye Sensor. Journal of Nanoscience and Nanotechnology, 2010, 10, 7730-7734.	0.9	1
222	Crystal structure of 8-methoxy-2-oxo-2H-chromene-3-carboxylic acid, C11H8O5. Zeitschrift Fur Kristallographie - New Crystal Structures, 2010, 225, 65-66.	0.1	1
223	Design and synthesis of novel symmetrical heptamethine cyanine chromophores. Fibers and Polymers, 2010, 11, 321-323.	1.1	1
224	Crystal structure of 4-(3,4-bis(2,5-dimethylthiophen-3-yl)- cyclopent-3-en-1-yl)benzaldehyde, C24H24OS2. Zeitschrift Fur Kristallographie - New Crystal Structures, 2010, 225, 606-608.	0.1	1
225	Novel triazacarbocyanine dye sensor synthesis: pH switching effect. Fibers and Polymers, 2011, 12, 976-978.	1.1	1
226	A Highly Selective Detection Properties of 1,3-Bisdicyanovinylindane for Hg ²⁺ Ion. Molecular Crystals and Liquid Crystals, 2011, 538, 320-326.	0.4	1
227	Synthesis and Optical Determination in Rhodamine-Based Chemosensors Toward Hg2+. Molecular Crystals and Liquid Crystals, 2012, 568, 117-124.	0.4	1
228	lonic comonomer effect of poly(N-isopropylacrylamide) copolymer containing D-Ï€-A type pyran-based fluorescent dye. Spectrochimica Acta - Part A: Molecular and Biomolecular Spectroscopy, 2012, 92, 33-36.	2.0	1
229	Crystal structure of 2,3-bis(2,4-dimethylthiazole-3-yl)thiophene, C14H14N2S3. Zeitschrift Fur Kristallographie - New Crystal Structures, 2013, 228, 95-96.	0.1	1
230	Design, Synthesis and Characteristics on Novel <i>D</i> - <i>Ï€</i> - <i>A</i> Dye Chromophore: Fluorochromism Effects. Journal of Nanoscience and Nanotechnology, 2013, 13, 1484-1487.	0.9	1
231	Fluorescence Quench of Arylmaleimide with a Substituted Anthracene. Molecular Crystals and Liquid Crystals, 2014, 600, 14-21.	0.4	1
232	Arylmaleimide Based Fluorescence On-Off Modulated by Ac2O/HCl. Molecular Crystals and Liquid Crystals, 2014, 597, 65-72.	0.4	1
233	Crystal structure of 7-(diethylamino)-2-oxo-2H-chromene-3- carbaldehyde, C14H15NO3. Zeitschrift Fur Kristallographie - New Crystal Structures, 2014, 229, .	0.1	1
234	The synthesis and spectral properties of a stimuli-responsive D-Ï€-A charge transfer dye based on phenol donor and isophorone acceptor moiety. Fibers and Polymers, 2015, 16, 1605-1610.	1.1	1

#	Article	IF	CITATIONS
235	A bright yellow emissive dye configured by attaching triarylamine to naphthalimide with ‒NHNË-bridge. Molecular Crystals and Liquid Crystals, 2016, 635, 172-180.	0.4	1
236	Optical properties of triphenylamine decorated with naphthalimide. Molecular Crystals and Liquid Crystals, 2017, 645, 1-9.	0.4	1
237	Photochromic behavior of 2,3-bis(2,5-dimethylthiophene-3-yl)thiophene-5-carbaldehyde oxime. Molecular Crystals and Liquid Crystals, 2017, 654, 123-130.	0.4	1
238	Photochromic behavior of triangle trithiophene with π-extension at the bridge unit. Molecular Crystals and Liquid Crystals, 2017, 654, 115-122.	0.4	1
239	Investigation of Fluorescent Optical Properties of Fluorine-Boron Cored Dye. Molecular Crystals and Liquid Crystals, 2018, 677, 27-33.	0.4	1
240	Interpretation of Absorption Spectra of Some Bisazomethine Dyes in a Crystalline State in Terms of Conformational Change and Exciton Interaction. Bulletin of the Chemical Society of Japan, 2018, 91, 1498-1505.	2.0	1
241	AgNP/crystalline PANI/EBPâ€compositeâ€based supercapacitor electrode with internal chemical interactions. Journal of Applied Polymer Science, 2019, 136, 48164.	1.3	1
242	Research and Development of Functional Colorants Materials. Korean Chemical Engineering Research, 2014, 52, 1-7.	0.2	1
243	Multichromic Dye Synthesis and Its Absorption Properties with Cyclodextrins. Molecular Crystals and Liquid Crystals, 2007, 472, 231/[621]-237/[627].	0.4	0
244	Selective Patterning of Quantum Dots on Functionalized Surface Using Polyelectrolyte Transfer. Molecular Crystals and Liquid Crystals, 2008, 492, 90/[454]-101/[465].	0.4	0
245	Selective Photoluminescence Dye Patterning on Light Stamping Lithography (LSL) PDMS molds. Molecular Crystals and Liquid Crystals, 2008, 491, 88-93.	0.4	0
246	Crystal structure of 3-carboxyethyl-7-diethylaminocoumarin, C16H19NO4. Zeitschrift Fur Kristallographie - New Crystal Structures, 2009, 224, 593-594.	0.1	0
247	Crystal structure of 2-(4-(diphenylamino)benzylidene)malononitrile, C22H15N3. Zeitschrift Fur Kristallographie - New Crystal Structures, 2009, 224, 493-494.	0.1	0
248	Self-Assembly Multi-Layer of 1,3-Bisdicyanovinylindane and Its Spectral Sensing Properties. Journal of Nanoscience and Nanotechnology, 2009, 9, 1160-1163.	0.9	0
249	Crystal structure of 3,3′-(4-(4-bromophenyl)cyclopent-1-ene-1,2-diyl)- bis(2,5-dimethylthiophene), C23H23BrS2. Zeitschrift Fur Kristallographie - New Crystal Structures, 2010, 225, 415-416.	0.1	0
250	Photophysical Switching Properties of Spironaphthoxazine-poly(styrene-sulfonic acid) Polyion Complex. Molecular Crystals and Liquid Crystals, 2010, 520, 151/[427]-157/[433].	0.4	0
251	Crystal structure of (Z)-2-amino-3-[(E)-2-(benzyloxy)-4-(diethylamino)- benzylideneamino]-2-butenedinitrile, C22H23N5O. Zeitschrift Fur Kristallographie - New Crystal Structures, 2011, 226, .	0.1	0
252	Crystal structure of (Z)-2-amino-3-[(E)-4-(dimethylamino)-2-ethoxybenzylideneamino]- 2-butenedinitrile, C15H17N5O. Zeitschrift Fur Kristallographie - New Crystal Structures, 2011, 226, .	0.1	0

#	Article	IF	CITATIONS
253	Crystal structure of 2-[4-(9H-carbazol-9-yl)benzylidene]-2,3- dihydroinden-1-one, C28H19NO. Zeitschrift Fur Kristallographie - New Crystal Structures, 2011, 226, .	0.1	0
254	Synthesis and Characterization of Colorimetric Metal Sensing Properties Based on Azo Chromophore Moiety. Molecular Crystals and Liquid Crystals, 2011, 538, 310-319.	0.4	0
255	Crystal structure of (2Z)-2-amino-3-[(E)-4-(diethylamino)-2-methoxybenzylideneamino]-2-butenedinitrile, C16H19N5O. Zeitschrift Fur Kristallographie - New Crystal Structures, 2012, 227, .	0.1	Ο
256	Crystal structure of (Z)-2-amino-3-[(E)-4-(diethylamino)-2- ethoxybenzylideneamino]-2-butenedinitrile, C17H21N5O. Zeitschrift Fur Kristallographie - New Crystal Structures, 2012, 227, .	0.1	0
257	pH Triggered Dye Chemosensor: Design, Synthesis and Optical Switching Properties. Molecular Crystals and Liquid Crystals, 2012, 566, 106-111.	0.4	0
258	pH triggered switching dye sensor based on furan and pyrone units. Fibers and Polymers, 2012, 13, 159-161.	1.1	0
259	Crys tal struc ture of 2,6-diiodo-8-phenyl-BODIPY, C19H17BF2I2N2. Zeitschrift Fur Kristallographie - New Crystal Structures, 2013, 228, 91-92.	0.1	0
260	Crystal structure of 2,6-diiodo-8-(3-iodophenyl)-phenyl-BODIPY, C19H16BF2I3N2. Zeitschrift Fur Kristallographie - New Crystal Structures, 2013, 228, 93-94.	0.1	0
261	Crystal structure of 5-(2,6-dimethyl-4H-pyran-4-ylidene)-1,3-dimethylpyrimidine- 2,4,6(1H,3H,5H)-trione, C13H14N2O4. Zeitschrift Fur Kristallographie - New Crystal Structures, 2013, 228, 97-98.	0.1	0
262	Crystal structure of 2-(4-diethylamino-2-hydroxyphenyl)-benzoxazole, C17H18N2O2. Zeitschrift Fur Kristallographie - New Crystal Structures, 2013, 228, 99-100.	0.1	0
263	Crystal structure of 2,3-bis(3'-methylthiophene-5'-carbaldehyde-2-yl) thiophene, C16H12O2S3. Zeitschrift Fur Kristallographie - New Crystal Structures, 2014, 229, 85-86.	0.1	0
264	Crystal structure of 5-bromo-2,3-bis(2',5'-dimethylthiophene-3-yl)- thiophene, C16H15BrS3. Zeitschrift Fur Kristallographie - New Crystal Structures, 2014, 229, .	0.1	0
265	Investigation of a Photochromic Diarylethene with Electron-acceptor Attached. Molecular Crystals and Liquid Crystals, 2015, 621, 102-111.	0.4	0
266	Synthesis of Isophorone based D-ï€-A Type Chemosensor for the Response of Hg ²⁺ . Molecular Crystals and Liquid Crystals, 2015, 622, 94-102.	0.4	0
267	Synthesis, characterization of symmetrical and unsymmetrical naphthoxy substituted metallophthalocyanines. Molecular Crystals and Liquid Crystals, 2017, 644, 249-256.	0.4	0
268	Emission behavior of a symmetrical sexthiophene. Molecular Crystals and Liquid Crystals, 2017, 644, 240-248.	0.4	0
269	Crystal structure of 5,5-difluoro-10-(4-fluorophenyl)-1,3,7,9-tetramethyl-5 <i>H</i> -4l4,5l4-dipyrrolo[1,2- <i>c</i> :2 $\hat{a}\in^2$,1 $\hat{a}\in^2$ - <i>f</i> - a $\hat{z}\hat{a}\in^2$ = 3 structure, C ₁₉ H ₁₈ B ₂ F ₃ N ₂ .][1,3,2]di	azaborinine
270	Zeitschrift Fur Kristallographie - New Crystal Structures, 2017, 232, 1013-1015, Crystal structure of 11-oxo-2,3,6,7-tetrahydro-1 <i>H</i> ,5 <i>H</i> ,11 <i>H</i> -pyrano[2,3- <i>f</i>]pyrido[3,2,1- <i>ij</i>]quinoline-	·10-carbalc	lehyde

 ⁻ a julolidine derivative, C₁₆H₁₅NO₃. Zeitschrift Fur Kristallographie - New Crystal Structures, 2017, 232, 991-992.

#	Article	IF	CITATIONS
271	Crystal structure of bis(4,4,5,5-tetramethyl-1,3,2-dioxaborolane)-9,9-dioctylfluorene, C ₄₁ H ₆₄ B ₂ O ₄ . Zeitschrift Fur Kristallographie - New Crystal Structures, 2017, 232, 987-989.	0.1	0
272	Synthesis, Spectral and Photophysical Properties of Anthracene Substituted Phthalocyanines; A Study as Polyurethane Electrospun Nanofibers. Journal of Nanoscience and Nanotechnology, 2018, 18, 1716-1722.	0.9	0
273	Highly fluorescent response of 4-(2,5-dimethylthiophen-3-yl)-2- hydroxyphenylbenzothiazole toward BF ₃ •Et ₂ O and Zn ²⁺ . Molecular Crystals and Liquid Crystals, 2018, 662, 132-138.	0.4	0
274	Thermochromic Properties of Fluorans in Solid State and Application in Acrylic Fiber as Thermal Indicator. Journal of Nanoscience and Nanotechnology, 2019, 19, 8013-8019.	0.9	0
275	Crystal structure of 2,7-diiodo-1,3,6,8-tetramethyl-bis(difluoroboron)-1,2-bis((1H-pyrrol-2-yl)methylene)hydrazine, C ₁₄ H ₁₄ 8 ₂ F ₄ 1 ₂ N ₄ . Zeitschrift Fur Kristallographie - New Crystal Structures. 2020. 235. 371-372.	0.1	0
276	Synthesis of Novel Oxazolidines and Study of Its Naked Eye CO ₂ Detecting Properties. Journal of Nanoscience and Nanotechnology, 2020, 20, 6428-6434.	0.9	0
277	Crystal structure of 2-phenylethynyl-1,3,6,8-tetramethylBOPHY (BOPHY =) Tj ETQq1 1 0.784314 rgBT /Overlock Kristallographie - New Crystal Structures, 2021, 236, 749-752.	10 Tf 50 5 0.1	07 Td (bis(dif 0
278	Refinement of crystal structure of β-phenylglutaric acid, C11H12O4. Zeitschrift Fur Kristallographie - New Crystal Structures, 2009, 224, 491-492.	0.1	0
279	Crystal structure of (4-(3,4-bis(2,5-dimethylthiophen-3-yl)- cyclopent-3-en-1-yl)phenyl)methanol, C24H26OS2. Zeitschrift Fur Kristallographie - New Crystal Structures, 2010, 225, 495-497.	0.1	0
280	Crystal structure of 2,3-bis(3-methylthiophen-2-yl)- benzothiophene 1,1-dioxide, C18H14O2S3. Zeitschrift Fur Kristallographie - New Crystal Structures, 2012, 227, .	0.1	0
281	Crystal structure of 2,3-bis(3-methylthiophen-2-yl)benzofuran, C18H14OS2. Zeitschrift Fur Kristallographie - New Crystal Structures, 2012, 227, .	0.1	Ο